DOI 10.5012/bkcs.2010.31.01.133

Visible Light Photoelectrocatalytic Properties of Novel Yttrium Treated Carbon Nanotube/Titania Composite Electrodes

Feng-Jun Zhang,[†,‡] Ming-Liang Chen,[†] Kan Zhang,[†] and Won-Chun Oh[†,*]

[†]*Department of Advanced Materials & Science Engineering, Hanseo University, Seosan, Chungnam 356-706, Korea*
[*]*E-mail: wc_oh@hanseo.ac.kr*
[‡]*School of Materials and Chemical Engineering, Anhui University of Architecture, Anhui Hefei, P. R. China, 230022*
Received September 21, 2009, Accepted November 27, 2009

Photoelectrocatalytic decolorization of methlene blue (MB) in the presence of two types of carbon nanotube/titania and yttrium-treated carbon nanotube/titania electrodes in aqueous solutions were studied under visible light. The prepared composite electrodes were characterized by X-ray diffraction, transmission and scanning electron microscopy, energy dispersive X-ray analysis, and photoelectrocatalytic activity. The photoelectrocatalytic performances of the supported catalysts were evaluated for the decolorization of MB solution under visible light irradiation. The results showed that yttrium incorporation enhanced the decolorization rate of MB. It was found that the photoelectrocatalytic degradation of a MB solution could be attributed to the combined effects caused by the photo-degradation of titania, the electron assistance of carbon nanotube network, the enhancement of yttrium and a function of the applied potential. The repeatability of photocatalytic activity was also tested. The presence of yttrium enhanced the hydrophillicity of yttrium-carbon nanotubes/titania electrode because more OH groups can be adsorbed on the surface.

Key Words: Yttrium-carbon nanotuble/titania, Electrode, Photoelectrocatalytic, Methylene blue, Visible light

Introduction

Titanium dioxide (TiO_2)-induced photocatalysis is an established advanced oxidation process for the treatment of contaminated aqueous and gaseous streams. However, poor adsorption capacity, formation of rapid aggregates in a suspension and also recycling difficulties restricted the utilization of bare TiO_2. Moreover, it can be excited only under illumination with UV light at wavelengths below 400 nm because of the large band gap (3.2 eV) for anatase TiO_2. Unfortunately, only *ca*. 4% of the solar radiation that reaches the Earth's surface exists in the UV region; indeed, more than 45% lies in the visible region.[1] Therefore, in practical applications, attempts have been made to support TiO_2 nanoparticles on porous adsorbent materials and to extend the light absorption of the photocatalysts to the visible region.[2-7]

Among these materials, carbon nanotubes (CNTs) have attracted much attention and have become a very active field of research.[8-13] CNTs, as a new class of nanomaterials, have been drawn to considerable attention for their applications as catalyst supports owing to their unique electrical properties, high chemical stability and high surface-to-volume ratio. Moreover, CNTs have a variety of electronic properties. They may also exhibit metallic conductivity as one of the many possible electronic structures. CNTs have a large electron-storage capacity (one electron for every 32 carbon atoms),[14] the ability of CNT can promote the electron-transfer reactions at carbon nanotubes modified electrodes.

On the other side, previous works[15-20] have also emphasized that photocatalytic (PC) activity of TiO_2 can be improved by doping of TiO_2 with transition metals. The study of Choi[15] studied 21 transition metal ions doped TiO_2 and found that when Fe^{3+}, Mo^{5+}, Ru^{3+}, Os^{3+}, Re^{5+}, V^{4+} and Rh^{3+} were used at 0.1 - 0.5%, a significant increase in the photo-reactivity of TiO_2 samples was achieved for both chloroform oxidation and reduction. In the review of Fox and Dulay,[16] oxidation states of elements were found to be important in a way that both trivalent and pentavalent ions behave as recombination centers for electron-hole pairs. Recently, it has been also demonstrated that the presence of heavy metals such as Pd, Au and Ag on TiO_2 can enhance the degradation efficiency of PC reactions.[17-20] Rare earth ions (La^{3+}, Eu^{3+}, Sm^{3+}, Nd^{3+}, Pr^{3+}) doped TiO_2 catalysts has also attracted much attention in PC processes owing to their high PC activities in the degradation of organic molecules.[21-22] A recent study investigated the photoactivity of yttrium incorporated TiO_2 supported ZSM-5 catalysts.[5] Yttrium incorporation enhanced the decolorization rate percentage of methyl orange. Lin and Yu reported the PC activities of mixtures of TiO_2 with Y_2O_3.[23] Their results revealed that mixtures of TiO_2 with Y_2O_3 (0.5 wt %) induce higher photoactivity than pure TiO_2 for the oxidation of acetone. In the study of Ismail,[24] Y_2O_3 particles were embedded into Fe_2O_3/TiO_2 mixed oxides by sol-gel method. This ternary mixed oxide resulted in a higher photooxidation rate for EDTA than pure TiO_2.

On the basis of these studies, we have attempted to prepare novel PC materials. This involves TiO_2 loading on the surface of CNTs modified by Y^{3+} ions, which, to the best of our knowledge, was not reported before. To explore the synergism induced after TiO_2 and Y_2O_3 nanoparticles are adsorbed on the CNTs surface, as prepared photocatalysts have been examined by using X-ray diffraction (XRD), surface area (BET) measurements, scanning electron microscopy (SEM) with energy dispersive X-ray analysis (EDX) techniques, and transmission electron microscopy (TEM). Performances of these new materials are tested for the PC decolorization of methylene blue (MB, $C_{16}H_{18}N_3S{\cdot}Cl{\cdot}3H_2O$) under visible light illumination. MB is a

water-soluble azo dye, produced in textile, printing, paper manufacturing, and pulp processing and pharmaceutical industries. It is a major water pollutant in these industries and release into the environment create real problems. It was selected because under anaerobic conditions it has the potential to produce more hazardous aromatic amines. Thus, MB is selected as the probe molecule in this study and its decolorization is controlled under the effect of yttrium ion content. Besides, recycling studies are performed to test the repeatability of the photocatalysts, and the hydrophilicity of the electrodes was also studied.

Experimental

Materials. Carbon nanotubes (CNTs) were selected as the support material. The CNTs (Multiwall nanotubes, diameter: ~20 nm, length: ~5 μm) were supplied from Carbon Nano-Material Technology Co., Ltd, Korea and used without further purification. The TNB (Ti $(OC_4H_7)_4$) as a titanium source for the preparation of composites was purchased from Acros Organics, New Jersey, USA. For the oxidization of the surface of the CNT, *m*-chloroperbenzoic acid (MCPBA) was used as an oxidized reagent; also purchased from Acros Organics, New Jersey, USA. Methylene blue was the analytical grade chemical and purchased from Duksan Pure Chemical Co., Ltd, Korea. Benzene (99.5%) was used as an organic solvent which was purchased from Samchun Pure Chemical Co., Ltd, Korea. Yttrium nitrate hexahydrate ($Y(NO_3)_3 \cdot 6H_2O$) was obtained from Daejung Chemicals & Metals Co., Ltd, Korea. The novolac typed polymer resin (PR) was supplied from Kangnam Chemical Co., Ltd, Korea. Reagent-grade solvents, benzene and ethyl alcohol, were purchased from Duksan Pure Chemical Co. and Daejung Chemical Co., Korea and used without further purification.

Preparation of Y-CNT composites. To begin preparing this experiment, the 2.0 g MCPBA as oxidizing agent was melted in 60 mL benzene. Then 0.6 g CNTs was put into the oxidizing agent, refluxed for 6 h, filtered and dried. The oxidized CNTs were added to nitrate solution containing $Y(NO_3)_3 \cdot 6H_2O$, of various concentration, and then the solutions were homogenized under reflux at 343 K for 2 h using a magnetic stirrer in a vial. After being heat treated at 773K for 1 h with a heating rate of 279 K/min, the Y treated CNT composites were obtained.

Preparation of Y-CNT/TiO_2 composite electrodes. The Y treated CNT composites were put into the mixing solution of TNB and benzene with a volume ratio of 4:16. Then the solutions were homogenized under reflux at 343 K for 5 h, while being stirred in a vial again. After stirred, the solutions transformed into Y-CNT/TiO_2 gels, and these gels were heat treated at 973 K for 1 h with a heating rate of 279 K/min. After cooling, the Y-CNT/TiO_2 composites were resulted. Then 0.4 g PR was added to the Y- CNT/TiO_2 composites, and the composites were pressed at a pressure of 250 kg/cm^2 in a mould with dimensions of 9.95 mm × 39.5 mm × 5.95 mm. The mixture was then heat treated at 673 K for 1 h. After cooling, the Y-CNT/TiO_2 composite electrodes were obtained. The preparation conditions and the nomenclatures of the samples are showed in Fig. 1 and Table 1.

Characterization of the Y-CNT/TiO_2 composites. XRD techinque was used for crystal phase identification and estimation of the anastase-to-rutile ratio. XRD patterns were obtained at room temperature with a diffractometer Shimata XD-D1 (Japan) using Cu Kα radiation. SEM was used to observe the surface state and porous structure of the Y-CNT/TiO_2 composites using a scanning electron microscope (JOEL, JSM-5200, Japan). EDX spectroscopy was used to measure the elemental analysis of the Y-CNT/TiO_2 composites. TEM (JEOL, JEM-2010, Japan) at an acceleration voltage of 200kV was used to investigate the size and distribution of the yttrium and titanium deposits on the CNT surface of various samples. TEM specimens were prepared by placing a few drops of the sample solution on a carbon grid. In order to test the hydrophilicity of the YCT series electrodes, the time of complete wetting for a drop of MB solution on the surface of electrode was determined. The hydrophilicity of the electrodes was studied in terms of the time of complete wetting measurement by a sessile drop method using a camera (SOK-DSC-T700, SONY).

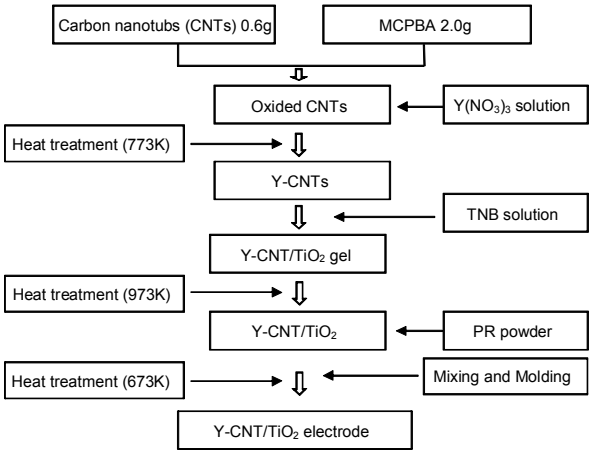

Figure 1. The flow chart of fabrication of Y-CNT/TiO_2 electrodes.

Table 1. Nomenclatures of Y-CNT/TiO_2 composites

Preparation method	Nomenclatures
2.0 g MCPBA + 0.6 g CNT + TNB 4 mL	YCT0
2.0 g MCPBA + 0.6 g CNT + $Y(NO_3)_3$ (0.01 M) + TNB 4 mL	YCT1
2.0 g MCPBA + 0.6 gCNT + $Y(NO_3)_3$ (0.015 M) + TNB 4 mL	YCT2
2.0 g MCPBA + 0.6 g CNT + $Y(NO_3)_3$ (0.020M) + TNB 4 mL	YCT3
2.0 g MCPBA + 0.6 gCNT + $Y(NO_3)_3$ (0.025M) + TNB 4 mL	YCT4

Photoelectrocatalytic (PEC) decolorization of MB. The PEC decolorization was performed by using Y-CNT/TiO_2 electrodes in a 100 mL glass container and then irradiating the system with visible light (8W, KLD-08L/P/N, FAWOO TECHNOLOGY), which was used at the distance of 100 mm from the solution in darkness box. Prior to illumination, the electrode was impregnated in the pristine MB solution in the dark for 30 min needed to achieve adsorption/desorption equilibrium. The counter electrode was artificial graphite (TCK, Korea), which dimension was 9.95 mm × 39.5 mm × 5.95 mm. The Y-CNT/TiO_2 elec-

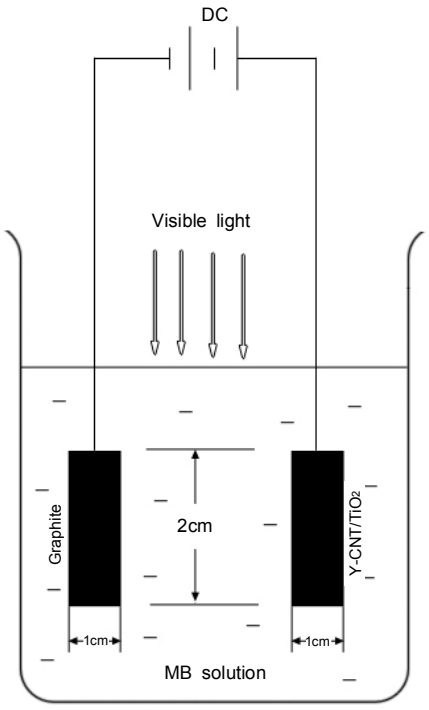

Figure 2. The sketch of PEC decomposition for MB solution with the Y-CNT/TiO_2 electrode.

Table 2. Surface areas of Y-CNT/TiO_2 composites.

Sample	S_{BET} (m^2/g)
YCT0	198
YCT1	172
YCT2	141
YCT3	129
YCT4	119

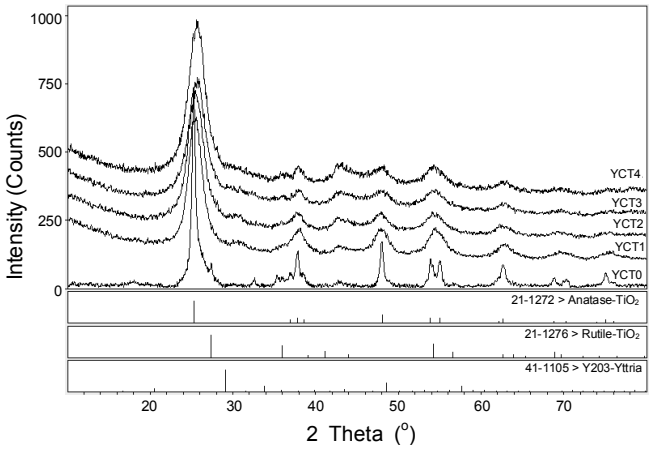

Figure 3. XRD patterns of Y-CNT/TiO_2 composites.

trodes were placed in 50 mL of 1.0×10^{-5} mol/L MB solution. The PEC degradation of MB was performed with voltage of 6.0 V and visible light (Fig. 2). The PEC activities of Y-CNT/TiO_2 electrodes were investigated using the PEC rate of MB solution, which was measured as function of time. The blue color of the solution faded gradually with time due to the adsorption and degradation of MB solution. And then the concentration of MB in the solution was determined as a function of irradiation time from the absorbance change at a wavelength of 660 nm. The decolorization rate of MB was calculated by the following equation:

$$\text{Decolorization (\%)} = (C_0 - C) / C_0 \times 100\%$$

Where C_0 is the initial concentration of MB and C is the concentration of MB after "t" minutes visible light irradiation.

Results and Discussion

Structure and morphology of Y-CNT/ TiO_2 composites. The values of BET surface areas of Y-CNT/TiO_2 composites are shown in Table 2. As shown in Table 2, the BET surface area of non-yttrium treated CNT/TiO_2 was 198, while the BET surface areas of yttrium treated CNT/TiO_2 composites decreased gradually from 172 to 119 m^2/g with an increase of $Y(NO_3)_3$ concentration. At the same addition of TNB, it was thought that the intensity of the Y particle aggregation increased with the increase of $Y(NO_3)_3$ concentration. These particles were heavily agglomerated to gather into a blocky-shaped particle. These results can be seen clearly from SEM images obtained from powdered Y-CNT/TiO_2 composites. The results showed that there is a decrease in the BET surface area of the Y-CNT/TiO_2 composites after formation of Y particles by $Y(NO_3)_3$ treatment. This was suggested that some porosity was developed during the heat treatment. It was thought that the composites are nano materials that include a lot of micropores. It was thought that there are two possible reasons. First, it could be attributed to the micropores being partly blocked by the formation of Y particles on the CNT/TiO_2 surface during heat treatment. Second, the BET surface area decreased due to the curing of polymer resin with heat treatment, which blocked the micropores and formed some new mesopores. It was possible that the phenol resin had coated some CNT/TiO_2 particles to form some larger composite particles during the curing process. As expected, the BET surface area is thought to decrease due to the blocking of the micropores by surface complexes introduced through the formation of Y-CNT/TiO_2 composites.

The XRD results for the catalyst samples are shown in Fig. 3. The structure of the non yttrium treated CNT/TiO_2 composites (YCT0) showed a mix of anatase and rutile crystals. It is well known that the crystal structure of the titanium dioxide is mainly determined by the heat treated temperature. The peaks at 25.3, 37.8, 48.0 and 62.5° (2θ) are the diffractions of (101), (004), (200) and (204) planes of anatase, indicating the developed CNT/TiO_2 composites existed in an anatase state. The peaks at 27.4, 36.1, 41.2 and 54.3° (2θ) belong to the diffraction peaks of (110), (101), (111) and (211) of rutile. Therefore, it can be concluded that the developed CNT/TiO_2 composites had a mixing structure of anatase and rutile crystals when annealed at 973 K. According to the published paper, if the anatase phase is

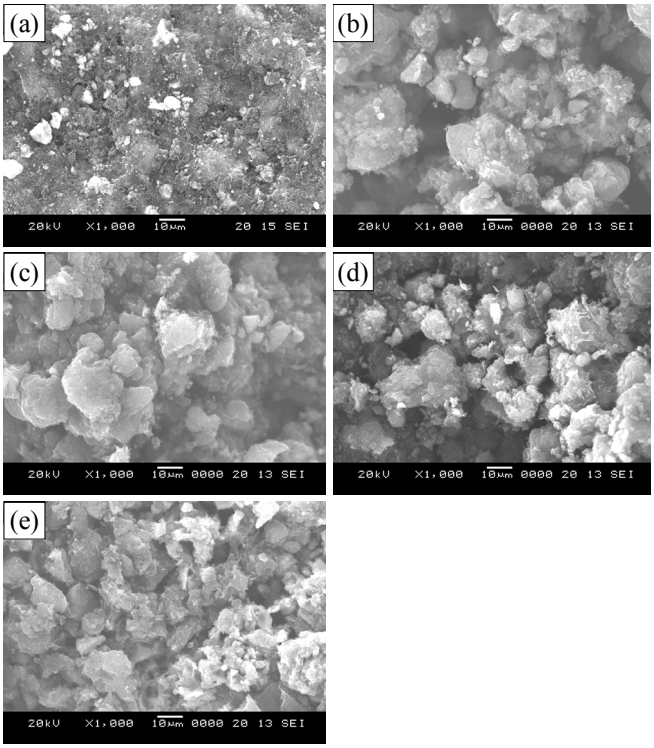

Figure 4. SEM images obtained from powdered Y-CNT/TiO_2 composites: (a) YCT0, (b) YCT1, (c) YCT2, (d) YCT3, (e)YCT4.

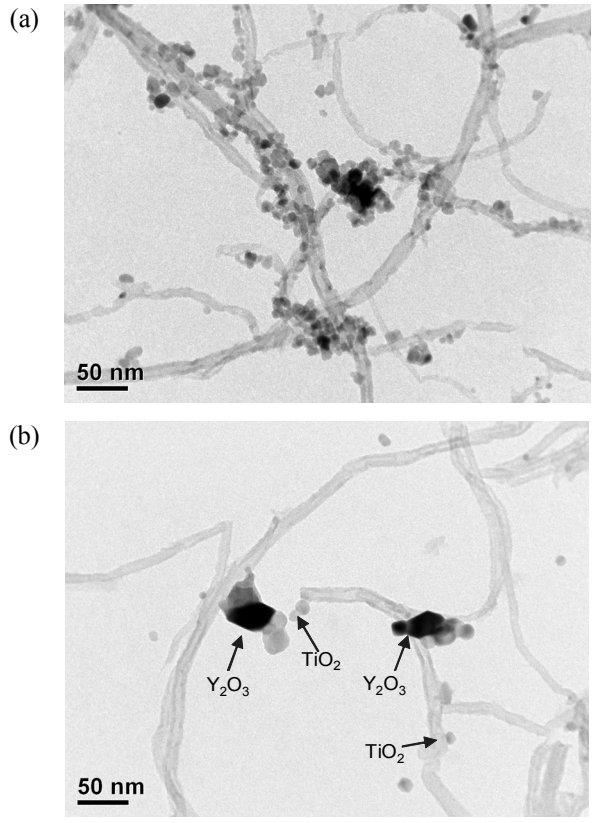

Figure 5. TEM micrographs obtained from powdered CNT/TiO_2 and Y-CNT/TiO_2 composites; (a) YCT0, (b) YCT2.

formed below 773 K, it starts to transformed into a rutile-type structure above 873 K, and then changes into a single phase of rutile at 973 K ~ 1173 K.[25] We have previously demonstrated that the crystallization phenomena in C/TiO_2 composites that are heat treated at 973K results in a mixed anatase-rutile structure.[26] Thus The XRD result obtained here is reasonable.

In the XRD patterns of Y-CNT/TiO_2 samples, formation of Y_2O_3 is searched owing to the variation of rare earth salt into rare earth oxides during the calcinations process. Although it is not clearly observable in Fig. 3, a new reflection at 29.2° (2θ) emerges and indicates characteristic (222) diffraction of Y_2O_3 particles. Additional Y_2O_3 diffractions (400), (411), (134) and (440) are obtained at 33.8, 35.9, 43.8 and 48.7° (2θ), respectively.[5] Intense peaks from anatase still appeared in the Y-CNT/TiO_2 composites and became broader than that of non-yttrium treated CNT/TiO_2 composite with increasing concentration of the Y $(NO_3)_3$ solution. Unfortunately, these high angle diffractions are complicated and not easily detected in the figure because of the overlapping of diffraction peaks attributed to TiO_2, Y_2O_3 and those of the CNTs support.

The micro-surface structures and morphology of the Y-CNT/TiO_2 composites were characterized by SEM (Fig. 4) and TEM (Fig. 5). Fig. 4 shows the macroscopical changes in the morphology of the Y-CNT/TiO_2 composites. As shown in Fig. 4, the TiO_2 particles were well attached to the surface of the CNT network, and the distribution was uniform. In the report of Zhang,[27] a good dispersion of small particles could provide more reactive sites for the reactants than aggregated particles. At the same time, the conductive of the CNT network can facilitate the electron transfer between the adsorbed dye molecules and the catalyst substrate.[28] It was beneficial for the enhancement of the PC activity of these composites. Moreover, yttrium particles were fixed on the surface of the CNT network in small clusters, and the distribution was not uniform. Moreover, we could not find the difference of the intensity of aggregation increased with the increase of Y $(NO_3)_3$ concentrations. These particles were heavily agglomerated to form blocky-shaped particle, and these results can be seen clearly in Fig. 4(b) to Fig. 4(d). These results are also confirmed by TEM inspection of the Y-CNT/TiO_2 composites. As shown in Fig. 5, for the CNT/TiO_2 composites, the TiO_2 particles were distributed uniformly outside surface of CNT tube; for the Y-CNT/TiO_2 composites, the TiO_2 particles were still distributed uniformly outside surface of CNT tube, Y particles were completely attached on the surface of the tube although this caused partial agglomeration to form blocky-shaped particle. However, in most cases, due to the capillary effect,[29-30] Y particles were formed outside the tubes, leading to poor synergic effect of the Y-CNT/TiO_2 composites.

Fig. 6 shows the EDX spectra of Y-CNT/TiO_2 composites prepared. From the EDX data, the main elements such as C, O, Ti and Y existed. The results of the EDX elemental microanalysis of the Y-CNT/TiO_2 composites are listed in Table 3. The contents of the yttrium component for YCT1, YCT 2, YCT 3 and YCT 4 are 0.9, 1.5, 1.8 and 2.1%, respectively. It can be expected that the contents of the yttrium component in the composites increased with an increase of $Y(NO_3)_3$ concentrations.

PEC decolorization of MB. Fig. 7 shows the PEC decolorization rate of MB for different Y-CNT/TiO_2 composite elec-

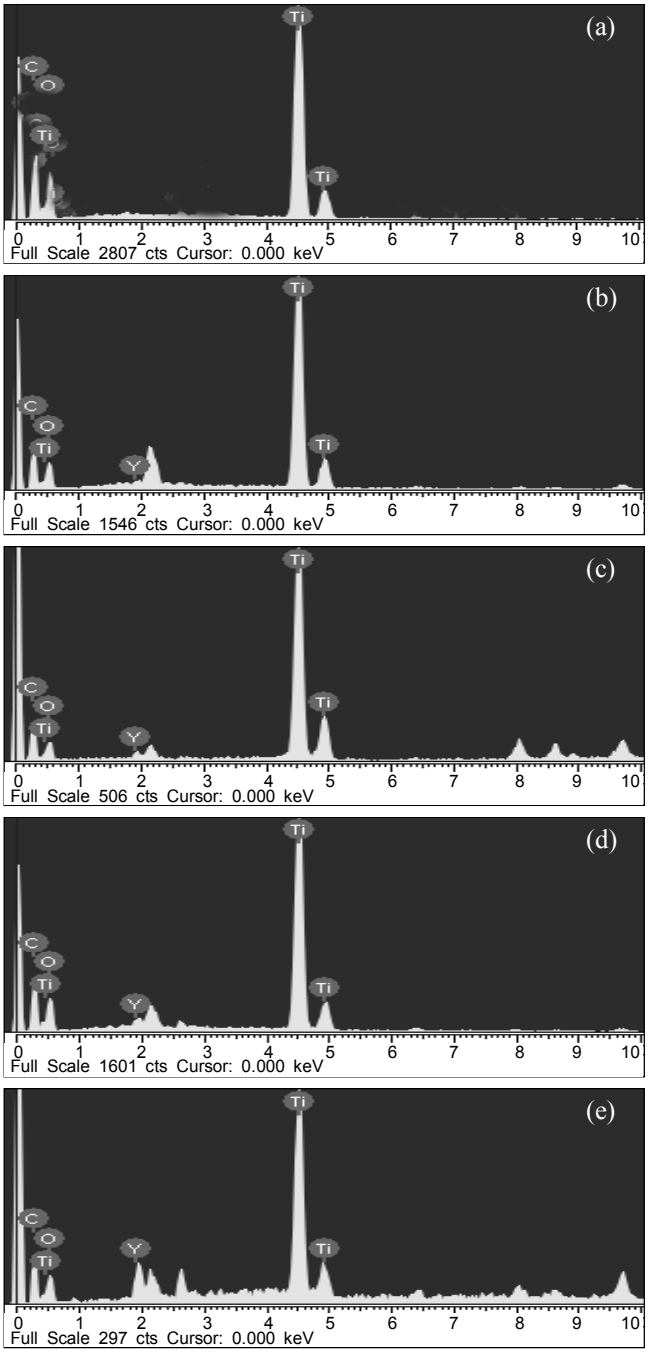

Figure 6. EDX elemental microanalysis of Y-CNT/TiO_2 composites: (a)YCT0, (b)YCT1, (c) YCT2, (d) YCT3, (e) YCT4.

Table 3. EDX elemental microanalysis of Y-CNT/TiO_2 composites

Samples	Element (wt. %)			
	C	O	Ti	Y
YCT0	21.0	36.0	43.0	0
YCT1	18.5	32.5	48.1	0.9
YCT2	20.2	29.8	48.5	1.5
YCT3	21.2	34.8	42.2	1.8
YCT4	22.7	30.8	44.4	2.1

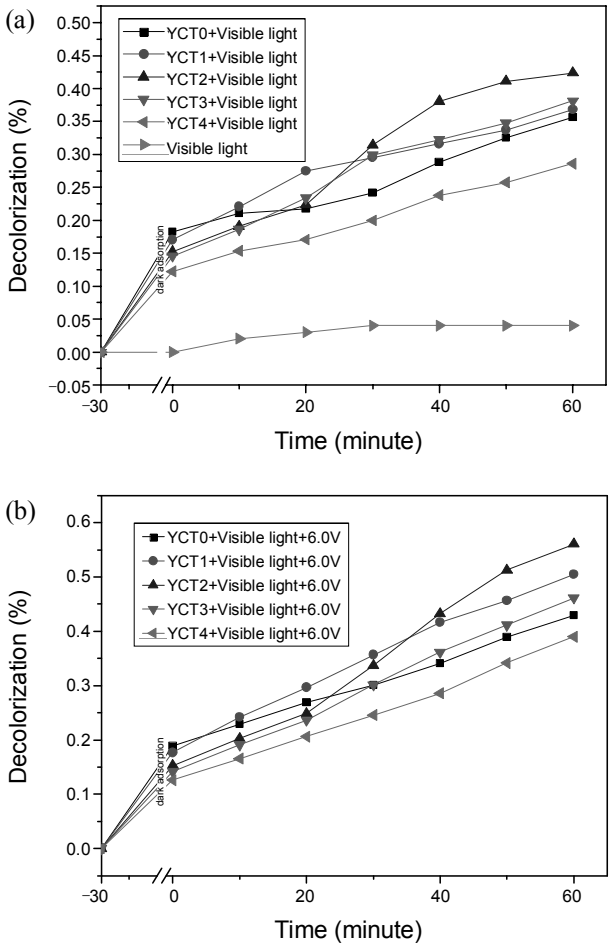

Figure 7. Effect of the photoelectrocatalytic decolorization rate of MB for different Y-CNT/TiO_2 composite electrodes: (a) under visible light irradiation, (b) in a function of the applied potential of 6.0V under visible light irradiation.

trodes under visible light irradiation with or without electron currents. Here we discussed three kinds of degradation process: 1). PEC: Visible light irradiation using the electrodes with a potential of 6.0V; 2). PC: Visible light irradiation using the electrodes; 3). P: Only visible light irradiation. From the results present in Fig. 7, comparing with CNT/TiO_2 and Y-CNT/TiO_2 composite electrodes, except YCT4, the PEC and PC effects of the Y treated CNT/TiO_2 composite electrodes were all better than that of non-Y treated CNT/TiO_2 in the irradiation time of 60 minutes. It was implied that the introduction of Y enhanced the PEC and PC degradation of MB solution. However, for the Y treated CNT/TiO_2 series, the PEC and PC degradation efficiency of the sample YCT2 is higher than that of the other samples in the irradiation time of 60 minutes. The electrocatalytic activity of Y particles for this reaction is dependent on various factors, which involves the size and dispersion of the particles, supporting materials and their surface conditions. In the case of YCT3 and YCT4, the Y particles were heavily agglomerated to gather into a blocky-shaped particle (see Fig.4 (d) and (e)), which leads to the significant reduction on its activity. It is well known that

the PEC activity will increase with an increase of Y content in a certain range. At the same time, the morphology of Y in the Y-CNT/TiO_2 composites is an important factor. Note that the optimization of PEC decolorization of MB using Y-CNT/TiO_2 composite electrodes will be studied in detail in another paper.

The repeatability of photoelectrocatalytst activity. To examine the stability of YCT2 electrode, recycling experiments are carried out (Fig. 8). For each new cycle, the photoelectrocatalyst is washed and calcined at 400 ^{o}C for 1 h by keeping other reaction conditions constant. After five cycles, the decolorization rate decreases only approximately 9%, from 56 to 47%. This indicates that the PEC activity of YCT2 electrode has repeatability. Similar results are obtained in system of yttrium incorporated TiO_2 supported ZSM-5.[5] The reduction in the decolorization rate among the cycles may be explained by the formation of by-products and their accumulation in the cavities and on the active surface sites of the electrode. It was thought that the result was due to the decrease of the electrode surface for both photon absorption and MB adsorption.

Visible light photo-induced hydrophilicity. In order to test the hydrophilicity of the YCT series electrodes, the time of complete wetting for a drop of MB solution on the surface of electrode was determined. If the time of complete wetting is short this means good wetting and the contact angle lower, which is good hydrophilicity. Changes of the MB solution complete wetting on the surface of Y-CNT/TiO_2 electrodes, induced by 8W visible light irradiation, are shown in Fig. 9. Indoor condition, the time of complete wetting for non yttrium treated CNT/TiO_2 electrode is about 8 minutes. It reduces with adding of yttrium and approaches 30 seconds for YCT2. However under visible light irradiation, the time of complete wetting falls from 8 to 6.5 minutes and from 5.5 to 3.5 minutes for YCT0 and YCT4, respectively. The time of complete wetting changes slightly for other electrodes due to the original times are lower. The results showed that YCT1, YCT2 and YCT3 have good hydrophilicity indoor or under visible light irradiation. It was considered that the mechanism of hydrophilicity is different from PC activity, the electrons and holes are still produced but they react differently. The electrons tend to reduce the Ti (IV) cations to Ti (III) state; the holes oxidize O_2^- anions. In this process oxygen atoms are ejected, creating oxygen vacancies. Water molecules can than occupy oxygen vacancies, producing adsorbed OH groups, which tend to make the surface hydrophilic. In spite of the different mechanisms of PC effect and hydrophilic effect, the correlation between the two is obvious. The photo-induced hydrophilicity of the electrode is closely related to the PC removal of organic substances from the electrode surface. The synergetic effect of photocatalysis and hydrophilicity can be understood as; because more OH groups can be adsorbed on the surface due to hydrophilicity, the PC activity is enhanced. So hydrophilicity can improve photocatalysis. On the other hand electrode surface can adsorb contaminated compounds which tend to convert the hydrophilic surface to the hydrophobic one. Photocatalysis can decompose the organic dirt on the electrode surface resulting in the restoration of hydrophilicity. This shows that photocatalysis can improve hydrophilicity and maintain this characteristic for long time. Y is supposed to enhance the hydrophilicity by taking an electron from Ti^{4+} to render it in Ti^{3+} state,

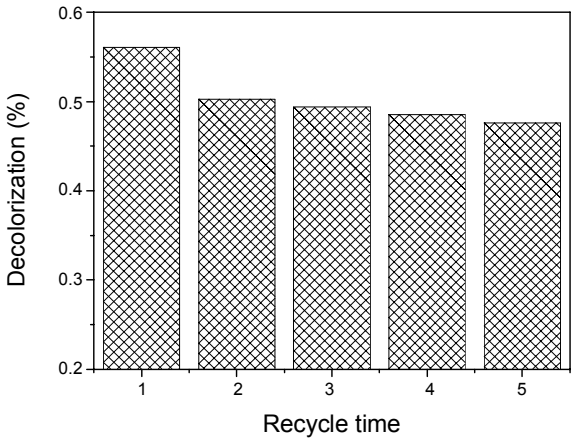

Figure 8. Effect of reuse of YCT2 electrode on the decolorization rate of MB in the aqueous solution with PEC reaction. (PEC: Visible light irradiation using the electrode with a potential of 6.0V)

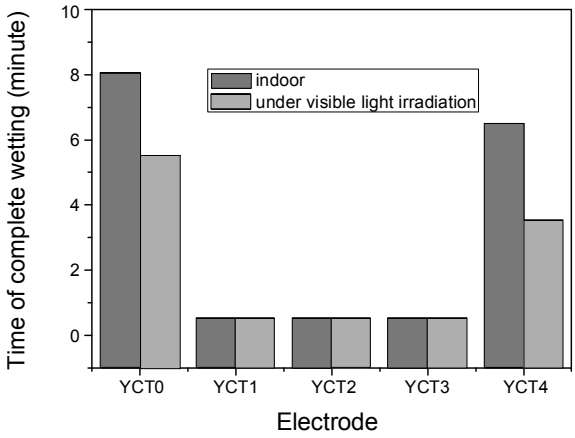

Figure 9. Visible light photo-induced change of the MB solution complete wetting on the surfaces of Y-CNT/TiO_2 electrodes.

while holes remaining at the valence band of TiO_2, thereby initiating the process for oxygen removal and hence hydrophilicity of the electrode.

Conclusion

In this study, we presented the fabrication and characterization of CNT/TiO_2 and Y-CNT/TiO_2 composite electrodes. The BET surface area of Y-CNT/TiO_2 composites decreased with an increase of Y component. XRD data revealed that the structure for the Y-CNT/TiO_2 composites showed a single anatase crystal phase. The TEM microphotographs of CNT/TiO_2 and Y-CNT/TiO_2 composites showed that TiO_2 particles were distributed uniformly in the CNTs network, and the Y particles were fixed on the surface of the CNTs, although they were partly aggregated. From the EDX data, the main elements such as C, O, Ti and Y existed. The Y-CNT/TiO_2 samples have a higher PEC and PC degradation efficiency than that of the non-Y treated CNT/TiO_2 sample. The results demonstrated that the PEC degradation of MB solution could be attributed to synergetic effects of the photo-degradation of TiO_2, the electron assis-

tance of the CNT network, the enhancement of Y and a function of the applied potential. The morphology of Y in the Y-CNT/TiO_2 composites is an important factor. A loss of the catalytic activity (9% in 60 minutes) of YCT2 electrode was found after its first use. Hydrophilicity and photoactivity arise due to two different mechanisms, but they go side by side i.e. if one increases the other also increases or vice versa, this is due to interfacial nature of the two processes.

Reference

1. Chen, L. C.; Ho, Y. C.; Guo, W. S. *Electrochim. Acta* **2009**, *54*, 3884.
2. Hamal, D. B.; Klabunde. K. J. *J. Colloid Interf. Sci*. **2007**, *311*, 514.
3. Carp, O.; Huisman, C. L.; Reller, *A. Prog. Solid State Chem*. **2004**, *32*, 33.
4. Wang, W. D.; Serp, P.; Kalck, P. *J. Mole. Catal. A Chem.* **2005**, *235*, 194.
5. Neren O¨ kte, A.; O¨ zge, Y. *Appl. Catal. B*: *Environ*. **2008**, *85*, 92.
6. Bhattachayya, A.; Kawi, S.; Ray, M. B. *Catal. Today* **2004**, *98*, 431.
7. Yoneyama, H.; Torimoto, T. *Catal*. *Today* **2000**, *58*, 133.
8. Fu, P. F.; Luan, Y.; Dai, X. G. *J. Mole. Catal*. *A*: *Chem*. **2004**, *221*, 81.
9. Oh, W. C.; Chen, M. L. *Bull. Korean Chem*. *Soc*. **2008**, *29*, 159.
10. Oh, W. C.; Jung, A. R.; Ko, W. B. *J. Ind. Eng. Chem*. **2007**, *13*, 1208.
11. Yang, S.; Zhu, W.; Li, X. *Catal. Commun*. **2007**, *8*, 2059.
12. Zhang, F. J.; Chen, M. L.; Oh, W. C. *Environ. Eng. Res*. **2009**, *14*, 32.
13. Zhang, F. J.; Chen, M. L.; Oh, W. C. *Mater. Res. Soc. Korea* **2008**, *18*, 583.
14. Kongkanand, A.; Kamat, P. V. *ACS. Nano*. **2007**, *1*, 13.
15. Choi, W.; Termin, A.; Hoffmann, M. R. *J. Phys. Chem*. **1994**, *98*, 13669.
16. Fox, M. A.; Dulay, M. T. *Chem. Rev*. **1993**, *93*, 341.
17. Xu, A.; Gao, W. Y.; Liu, H. Q. *J. Catal*. **2002**, *207*, 151.
18. Jing, L. Q.; Sun, X. I.; Xin, B. F. *J. Solid State Chem*. **2004**, *177*, 3375.
19. Shankar, M. V.; Cheralthan, K. K.; Arabindoo, B. *J. Mole. Catal*. **2004**, *223*, 195.
20. Shankar, M. V.; Anandan, S.; Venkatachalam, N. *Chemosphere* **2006**, *63*, 1014.
21. Zhang, Y. H.; Zhang, H. X.; Xu, Y. X. *J. Mater. Chem*. **2003**, *13*, 2261.
22. Liang, C. H.; Li, F. B.; Liu, C. S. *Dyes Pigments* **2008**, *76*, 477.
23. Lin, J.; Yu, J. C. *J. Photochem. Photobiol. A*: *Chem*. **1998**, *116*, 63.
24. Ismail, A. A. *Appl. Catal. B*: *Environ*. **2005**, *58*, 115.
25. Inagaki, M.; Hirose, Y.; Matsunaga, T. *Carbon* **2003**, *41*, 2619.
26. Oh, W. C.; Chen, M. L. *J. Ceram. Process Res*. **2008**, *9*, 100.
27. Zhang, X. W.; Zhou, M. H.; Lei, L. C. *Carbon* **2005**, *43*, 1700.
28. Christensen, P. A.; Curtis, T. P.; Egerton, T. A. *Appl. Catal. B*: *Environ*. **2003**, *41*, 371.
29. Ugarte, U.; Chatelain, A.; De Heer, W. A. *Science* **1996**, *274*, 1897.
30. Ajayan, P. M.; Iijima, S. *Nature* **1996**, *361*, 333.